

## Recent results on saturation and CGC

K. Itakura<sup>a</sup>

<sup>a</sup> Institute of Particle and Nuclear Studies, High Energy Accelerator Research Organization (KEK), 1-1 Oho, Tsukuba, Ibaraki 305-0801, JAPAN.

I discuss recent results on the Color Glass Condensate which is a dense saturated gluonic state and appears as the universal picture of hadrons or nuclei at very high energies.

### 1. Introduction

Since the previous Quark Matter conference held in January 2004, we have seen a very rapid progress in understanding the physics of the Color Glass Condensate (CGC). There are mainly three reasons for this sudden progress: First, because new experimental results reported by the BRAHMS collaboration in QM04 strongly suggested the existence of the CGC. Good experiments always stimulate theorists and lead to theoretical developments. Second, because a new interpretation of the Balitsky-Kovchegov (BK) equation was proposed based on the analogy with reaction-diffusion dynamics. This gave us an intuitive understanding about the emergence of the saturation scale and the geometric scaling. Third, because it has been recognized that the BK equation is not complete in that it does not contain the effects of pomeron loops. This fact drove people to think hard about the physics beyond the BK equation. These three reasons are all triggers for the recent rapid progress. Indeed all of such activities happened within one or two years and some of them are still going on now. Many papers were produced during this short period. Thus, instead of covering all these activities, I will have to focus on only a few subjects in this talk. But, in order to make this talk as self-contained and comprehensive as possible, I will start with presenting our motivation why we study the CGC. Then I will explain the properties of our basic equation, the BK equation, in an intuitive way based on the analogies with population dynamics and reaction-diffusion dynamics.

#### 1.1. Color Glass Condensate as the high energy limit of QCD

The most fundamental and general question which motivated our activities is "What is the high-energy limit of QCD?" Here "high-energy limit" is meant for the limit of large scattering energy. As I explain below, there are enough reasons to believe that there exists qualitatively different picture for hadrons or nuclei when the scattering energy is asymptotically large. If it indeed exists, then the natural questions to be asked next by experimentalists and theorists may be, respectively, "Is it already seen in experiments at current energy?", and "How can we treat it? Can we use weak-coupling techniques?". These are the questions which we always have in our minds, and I will give answers to them in this talk. But, before doing so, let me first introduce two important experimental results which suggest the possible form of the high energy limit of QCD.

The first one is  $F_2(x, Q^2)$  structure function measured in deep inelastic scattering (DIS) at HERA [ 1]. The data show steep rise of  $F_2$  with decreasing  $x$ , which is ordinarily attributed to the increase of gluon density in a proton. Since going smaller  $x$  corresponds to increasing scattering energy, this implies that high density gluons can be seen in a highly accelerated proton. The next experimental result is the hadronic cross section at high energy. For example, total cross section for proton-proton scattering, that is available in the particle data book [ 2] for quite a wide range of energy, shows very slow growth with increasing energy. The most recent PDG followed the analyses by the COMPETE collaboration [ 3] and adopted the parametrization  $\sigma^{ab} = Z^{ab} + B \ln^2(s/s_0) + \dots$  whose second term gives the leading energy dependence of the data. Here,  $\sigma^{ab}$  is the (total) cross section for scattering between hadrons  $a$  and  $b$ ,  $Z^{ab}$  is just a constant, and  $s$  is the total energy squared. This form of the cross section is motivated by the Froissart bound which is a result of unitarity in the  $S$ -matrix theory. Also important is the fact that the coefficient  $B$  is universal, that is, independent of the species of scattering hadrons.

These two experimental results suggest that the limit of large scattering energy will be significantly different from the ordinary picture of hadrons, and will be characterized by *many gluons, unitarity, and universal picture*. In a frame where most of the total momentum is carried by the target, the target can be treated as a state having these three properties. Recently, this new state of matter which becomes relevant at high energy has been named as the Color Glass Condensate [ 4]. This name is after the following observations. First of all, it is made of gluons ("small- $x$  gluons") which have **color** and carry small fractions  $x \ll 1$  of the total momentum of the hadron. Next, these small- $x$  gluons are created by slowly moving color sources (partons with larger  $x$ ) which are distributed randomly on the two dimensional disk (the Lorentz contracted hadron). This situation is very similar to that of a **glass** whose constituents are disordered and appear to be frozen in short time scales. Lastly, the density of small- $x$  gluons becomes very large until it is saturated to some value. Typically the occupation number of gluons is of  $\mathcal{O}(1/\alpha_s) \gg 1$  at saturation, which is like a **condensate** of bosons. As the scattering energy is increased, the hadrons undergo multiple production of small- $x$  gluons, and eventually become the CGC. Therefore, one can say that *the high energy limit of QCD is the Color Glass Condensate*. Note that this claim is as correct as the statement about the other limits of QCD: high temperature/density limit of QCD is the QGP/color superconductor, which now everyone believes true. In the same sense, if one goes to high energy limit in QCD, one will necessarily encounter the CGC. Note also that these three different limits allow for weak-coupling descriptions powered by sophisticated resummation schemes.

## 2. The Balitsky-Kovchegov equation

Properties of the CGC are specified by correlation functions of gluons (or Wilson lines made of gluon fields), and change of the CGC with increasing energy is determined by "evolution" equations for these correlation functions. In particular, the 2-point correlation function determines basic properties of the CGC and the evolution for this is given by a nonlinear integro-differential equation called the *Balitsky-Kovchegov (BK) equation* [ 5]. Physically, the 2-point correlation function corresponds to the *scattering amplitude*  $\mathcal{N}$  of a "color dipole" off the CGC, and can be identified with the gluon number in the target (CGC) when the gluon field is not strong. Therefore, the BK equation describes

the change of gluon number in a target under the change of scattering energy. Explicitly, it is given by ( $\bar{\alpha}_s = \alpha_s N_c / \pi$ )

$$\begin{aligned} \frac{\partial}{\partial Y} \mathcal{N}_Y(x_\perp, y_\perp) &= \frac{\bar{\alpha}_s}{2\pi} \int d^2 z_\perp \frac{(x_\perp - y_\perp)^2}{(x_\perp - z_\perp)^2 (y_\perp - z_\perp)^2} \\ &\times \{ -\mathcal{N}_Y(x_\perp, y_\perp) + \mathcal{N}_Y(x_\perp, z_\perp) + \mathcal{N}_Y(z_\perp, y_\perp) - \mathcal{N}_Y(x_\perp, z_\perp) \mathcal{N}_Y(z_\perp, y_\perp) \}, \end{aligned} \quad (1)$$

where  $\mathcal{N}_Y(x_\perp, y_\perp)$  is the scattering amplitude of the  $q\bar{q}$  dipole with  $x_\perp$  and  $y_\perp$  being the transverse positions of the quark and the antiquark, and  $Y \sim \ln s$  is the rapidity.

As a result of extensive investigation of this equation both in analytic [ 6, 7, 8] and numerical [ 9] methods, it turned out that there exists saturation regime whose borderline is given by the *saturation momentum*  $Q_s(x, A)$  so that gluons having transverse momenta lower than  $Q_s(x, A)$  are saturated. Intuitively, it corresponds to (inverse of) the typical transverse size of gluons when the transverse plane of the target is filled with gluons. Since the saturation momentum depends upon energy (or  $x$ ) and number of nucleons  $A$  as  $Q_s^2(x, A) \propto A^{1/3} (1/x)^\lambda$  with  $\lambda \simeq 0.3$  [ 10], it grows with increasing energy ( $x \rightarrow 0$ ) or for large nuclei, and the kinematical region for saturation expands. This particular dependence upon  $x$  and  $A$  leads to an interesting observation that the saturation scales for the  $ep$  DIS at HERA and for the Au-Au collisions at RHIC are of the same order  $Q_s(x \sim 10^{-4}, A = 1) \simeq Q_s(x \sim 10^{-2}, A \sim 200)$ . Therefore, if one finds saturation effects in the HERA data, then there is enough reason to expect similar things in the RHIC data. Since most of the gluons have their transverse momenta around  $Q_s(x, A)$ , the weak-coupling treatment becomes better and better with increasing energy  $\alpha_s(Q_s) \ll 1$ . Also, the solution at saturation regime (at large rapidities) is robust against the small perturbation of the initial condition specified at lower rapidities. Thus, the saturation regime appears to show a universal behavior. Lastly, the solutions to the BK equation exhibit new scaling phenomena called *geometric scaling* [ 6] which naturally comes out due to the presence of a saturation momentum, and is also observed in experimental data in a beautiful way [ 11]. These properties can be intuitively understood by the analogy with population dynamics and reaction-diffusion dynamics, as I explain below.

## 2.1. Global energy dependence – the population dynamics

In order to qualitatively understand what happens in the BK equation, let us ignore the transverse dynamics for the time being. This simplification allows us to find an interesting analogy with the problem of population growth [ 12]. Long time ago, Malthus discussed that growth rate of population should be proportional to the population itself, and proposed a simple linear equation for the population density  $N(t)$ :

$$dN(t)/dt = \alpha N(t). \quad (2)$$

Its solution  $N(t) = N_0 e^{\alpha t}$  shows exponential growth known as the "population explosion." Of course everyone knows that such an abnormal future is not our own. Indeed, as the number of people increases, this equation fails to describe the actual growth because various effects such as lack of foods help to reduce the speed of growth. One can simulate such effects by replacing the growth constant  $\alpha$  by  $\alpha(1 - N)$  which decreases with increasing  $N$ . This yields the famous *logistic equation* which was first proposed by Verhulst:

$$dN(t)/dt = \alpha (N(t) - N^2(t)). \quad (3)$$

Compared to eq. (1), this equation has a nonlinear term with a minus sign. In Fig. 1, we show the solutions to eq. (3) with different initial conditions at  $t = 0$ , together with the corresponding solutions to the linear equation (2). We can learn much from this simple result. First of all, at early time  $t \ll 1/\alpha$ , the solution shows rapid exponential growth as in the linear case. However, as  $N(t)$  grows, the nonlinear term ( $\sim N^2$ ) becomes equally important, and the speed of growth is reduced. Eventually at late time, the solution approaches to a constant (*saturate!*) which is determined by the asymptotic condition  $dN/dt = 0$ . Next, note that two solutions of the logistic equation with different initial conditions approach to each other, and converge to the same value, while deviation of two solutions of the linear equation expands as time goes. Namely, in the logistic equation, the initial condition dependence disappears as  $t \rightarrow \infty$ . In other words, the solutions to the logistic equation show *universal behavior* at late time.

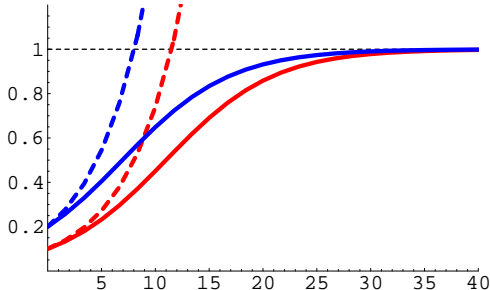


Figure 1. Comparison of the solutions  $N(t)$  to eq. (3) [solid lines] and eq. (2) [dashed lines], with different initial conditions at  $t = 0$ . The figure shows saturation and initial-condition independence of the logistic solution at late time.

The similarity of these equations to our problem is rather trivial:  $N$  and  $t$  correspond to the scattering amplitude  $\mathcal{N}$  and the rapidity  $Y$ , respectively. When the gluon density is not so high, change of the gluon number (scattering amplitude) with increasing rapidity is described by the BFKL equation [13]:

$$\frac{\partial}{\partial Y} \mathcal{N}_Y(k_\perp) = \bar{\alpha}_s K_{\text{BFKL}} \otimes \mathcal{N}_Y(k_\perp), \quad (4)$$

where  $\mathcal{N}_\tau(k)$  is the momentum representation of the dipole scattering amplitude, and  $\bar{\alpha}_s K_{\text{BFKL}}$  is the kernel representing the probability of splitting of one dipole into two. This is essentially a linear equation, and its solution at asymptotically large  $Y$  shows exponential growth  $\mathcal{N}_Y(k) \sim \exp\{(4\bar{\alpha}_s \ln 2) Y\}$ . This result is an analog of the population explosion in the population dynamics. This solution, however, violates the unitarity bound for the amplitude ( $\mathcal{N}_\tau \leq 1$ ) and the BFKL equation must be modified so as not to violate the unitarity. In fact, what is missing in the BFKL equation is the *recombination process* of two gluons into one, which cannot be ignored when the gluon density is high. Note that this process effectively reduces the speed of growth. Once this is included, the BFKL equation is replaced by the BK equation (1). In the momentum space, it can be schematically represented as

$$\frac{\partial}{\partial Y} \mathcal{N}_Y(k_\perp) = \bar{\alpha}_s K_{\text{BFKL}} \otimes \left( \mathcal{N}_Y(k_\perp) - \mathcal{N}_Y^2(k_\perp) \right). \quad (5)$$

Notice the similarity in the structure with the logistic equation (3). Therefore, it is now easy to understand that the solution to the BK equation shows (i) *saturation* and *unitarization* of the gluon number and (ii) *universality* that the solution at very large rapidity becomes independent of the initial condition.

## 2.2. Traveling waves in the reaction-diffusion dynamics

The intuitive picture presented above is not just an analogy, but can be justified as the limiting case of the remarkable observation made by Munier and Peschanski [14]. In a series of papers, they established the following fact:

**Fact:** *Within a reasonable approximation, the BK equation in the momentum space (5) can be rewritten as the FKPP (Fisher, Kolmogorov, Petrovsky, Piscounov) equation*

$$\partial_t u = \partial_x^2 u + u - u^2 \quad (6)$$

where  $t \sim Y$ ,  $x \sim \ln k_{\perp}^2$  and  $u(t, x) \sim \mathcal{N}_Y(k_{\perp})$ .

The FKPP equation is a famous equation in non-equilibrium statistical physics covering many interesting phenomena such as directed percolation, pattern formation, spreading of epidemics, etc., and has been investigated in great detail. The dynamics described by this equation is called the *reaction-diffusion dynamics* because the last two terms represent "reaction" part which is equivalent to the right-hand side of the logistic equation (3) with  $\alpha = 1$ , while the first term represents the diffusion. (Now it is easy to understand that the logistic equation (3) indeed comes out under the constant mode approximation  $\partial u / \partial x = 0$ .) Therefore, the solution to this equation is determined due to the interplay between these two effects. As we saw before, the logistic part induces the transition from unstable (exponentially growing) state to stable (saturated) state at some position  $x$ . On the other hand, the stable region expands due to the effect of diffusion. Therefore, it is very natural that the FKPP equation has a *traveling wave* solution. Typical traveling wave solutions at different time  $t$  and  $t' > t$  are shown in Fig. 2.

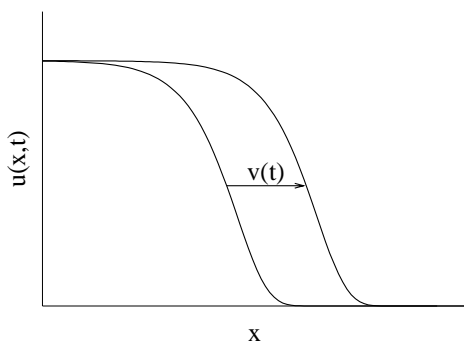


Figure 2. Traveling wave solutions to the FKPP equation (6) at different time  $t$  (left) and  $t' > t$  (right) as a function of  $x$ . (Figure by courtesy of R. Enberg)

There are two facts about this traveling wave solution, both of which are significantly relevant to the saturation physics:

**Fact I :** *For a traveling wave solution, one can define the position of a "wave front"  $x(t) = v(t)t$ , irrespective of the details of the nonlinear effects.*

**Fact II:** *At late time, the "shape" of a traveling wave is preserved during its propagation, and the solution becomes only a function of  $x - vt$ .*

Let us translate these facts into the language of saturation physics. Fact I is one of the most important facts for the saturation physics because *the position of the wave front is nothing but the saturation scale  $x(t) \sim \ln Q_s^2(Y)$* . By definition, the position of the wave front locates at the transition point from the unstable to stable regimes. On the other hand, the saturation scale is defined as the boundary between saturated (stable) and non-saturated (unstable) regimes. Therefore it is quite natural that the position of the wave

front corresponds to the saturation scale. What is more important is that the saturation scale can be determined irrespective of the nonlinear effects. This is again consistent with our knowledge that the energy dependence of the saturation scale can be determined by the linear BFKL evolution.

Fact II itself implies that the solution  $u(t, x)$  which is originally a function of position  $x$  and time  $t$  will show a scaling that it depends only on a specific combination of two variables  $x - x(t)$ . Within the saturation language, one finds that this phenomenon corresponds to the *geometric scaling* where the scattering amplitude becomes a function of a particular combination of transverse momentum  $k_\perp$  and some function of  $x$ , namely, the scaling variable is  $x - x(t) \sim \ln^2 k_\perp^2 / Q_s^2(Y)$  and thus  $\mathcal{N}_Y(k) = f(k_\perp^2 / Q_s^2(Y))$ . This scaling holds very well in a deeply saturated regime, where the profile of the solution does not change. This again implies the universality of the saturation regime. On the other hand, as one departs from the saturation regime (or the wave front) toward dilute (unstable) regime, the effect of saturation becomes weaker and weaker and eventually disappears, and the solution ceases to show the scaling. Still, one can approximately see the scaling if one stays close to (but outside of) the saturation boundary. One can estimate the upper limit of the transverse momentum squared below which the solution will show the scaling. Namely, the scaling is approximately seen in the following window (referred to as the extended scaling regime) [ 7]:

$$Q_s^2(x) \lesssim Q^2 \lesssim Q_s^4(x) / \Lambda_{\text{QCD}}^2. \quad (7)$$

This upper limit is roughly consistent with the experimental data at HERA [ 11]. The geometric scaling is indeed observed up to  $Q^2 \sim 100 \text{GeV}^2$  while the saturation scale at HERA is estimated as about  $Q_s^2 \sim 1 \text{GeV}^2$  at  $x \sim 10^{-4}$ .

Hence we recognized that there is a qualitatively different regime in between the CGC and dilute regimes. The theoretical status at this point for a proton as seen in DIS is summarized in Fig. 3.

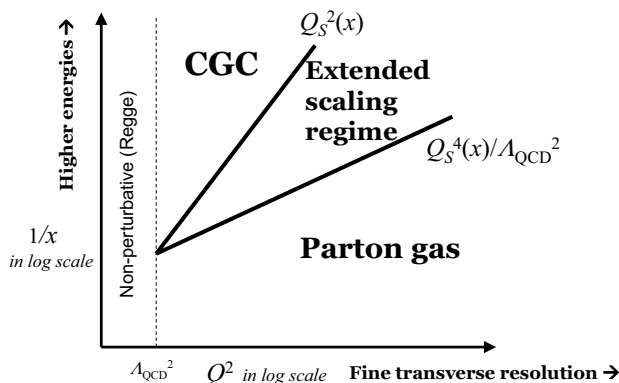


Figure 3. "Phase diagram" of a proton as seen in deep inelastic scattering.

### 3. Recent progress in phenomenology

Our understanding of the CGC has been deepened partly (in fact, largely) due to the experimental results at HERA and RHIC. Below I briefly explain some of the attempts to describe/understand the experimental data from the viewpoint of the CGC.

### 3.1. DIS at HERA

DIS at small  $x$  is the cleanest process for measuring saturation effects in gluon distribution of the proton. Starting from the pioneering work by Golec-Biernat and Wüsthoff [15], there are several attempts to describe the HERA DIS data [1] in the context of gluon saturation. Here let me briefly explain the "CGC fit" [16] which is one of the most successful fits of the small  $x$  data based on QCD. The CGC fit is constructed so as to contain two approximate solutions to the BK equation, which are valid in the saturation and BFKL regimes, respectively. In particular, the solution in the linear BFKL regime shows the geometric scaling and its (small) violation. With only three parameters, the CGC fit provides a very nice fit for the  $F_2$  structure function with  $x < 10^{-2}$  and in  $0.045 < Q^2 < 45 \text{ GeV}^2$ . From the fit, the saturation scale was determined as

$$Q_s^2(x) = (1 \text{ GeV})^2 (x_0/x)^\lambda, \quad \text{with } x_0 = 0.26 \times 10^{-4}, \lambda = 0.25. \quad (8)$$

Meanwhile, it turned out that this fit works reasonably well even for other observables such as  $F_2^{\text{diff}}$ ,  $F_L$  and the vector meson production [17, 18]. Precise determination of the saturation scale is also important for the analysis involving nuclei because one can determine the saturation scale for the nucleus by using the result for a proton.

### 3.2. Au-Au collisions at RHIC

The CGC provides the initial condition for the heavy ion collision. Information of the initial state could still be seen in the final observed data. It should be noticed that most of the produced particles have small momenta less than 1 GeV which is of the same order as  $Q_s$  in RHIC. This observation suggests that effects of saturation may be visible in bulk quantities such as the multiplicity. Indeed, the CGC results [19, 20] for the pseudorapidity and centrality dependences of the multiplicity are in good agreement with the data.

### 3.3. Deuteron-Au collisions at RHIC

Going to forward rapidities in a p-A collision corresponds to probing a nuclear wavefunction at smaller  $x$ , which should exhibit saturation with decreasing  $x$ . Thus, this is one of the best places to search for the CGC or the effects of quantum evolution [21]. For example, such effects should be measured in the nuclear modification factor, and this was indeed done by the BRAHMS experiment in the deuteron-Au collisions at RHIC [22]. The experimental data show *enhancement* of the ratio at mid-rapidity (the Cronin effect) and *suppression* at forward rapidities. Such global behavior is qualitatively consistent with the predictions made by the CGC [23, 24]. After the data was announced, many publications followed to confirm that this phenomena are indeed due to the saturation and CGC (for a review, see Ref. [25]). For instance, detailed analytical investigation of the ratio<sup>1</sup> was performed by Iancu, Triantafyllopoulos, and myself [26] and it has been clarified that the Cronin effect is due to multiple Glauber-Mueller scattering and re-distribution of gluons, both of which are properly described by the McLerran-Venugopalan model (classical saturation model without evolution), and that the high  $p_\perp$  suppression is induced by the mismatch of the evolution speed between the proton (deuteron) and the nucleus. The nucleus is closer to saturation and thus evolves slower than the proton. Quantitative

---

<sup>1</sup>More precisely, a ratio of the nuclear wavefunction to the proton wavefunction scaled up by  $A^{1/3}$ , which shows very similar behaviors as the nuclear modification factor.

results are also available. Kharzeev, Kovchegov, and Tuchin have computed the nuclear modification factor within the framework of the CGC [27], and found rather good agreement with the BRAHMS data. Very recently, there was an important progress: Dumitru, Hayashigaki, and Jalilian-Marian recognized that including the DGLAP evolution in the *projectile* side significantly improves the transverse spectra of the produced particles [28]. Up to now, their result seems to be the best one for this observable. Also important is the fact that the averaged value of  $x_A$  (the fraction of gluon momentum coming from the target nucleus) is small enough  $\langle x_A \rangle \sim 10^{-3}$  for the  $2 \rightarrow 1$  kinematics, which is highly contrasted with the results  $\langle x_A \rangle \sim 10^{-2}$  for the standard  $2 \rightarrow 2$  kinematics with the leading twist shadowing [29]. Therefore, our framework gives a consistent description of the deuteron-Au scattering.

Lastly, various observables have been computed and found to show suppression due to saturation. They include dileptons and photon productions [30] for the electro-magnetic probes,  $q\bar{q}$  or heavy meson productions [31], jet azimuthal correlations [32], etc. Note that EM probes are important in that they are less ambiguous because the process does not contain fragmentation functions.

So far, we have understood many things within the framework of the CGC, but in fact there are several other approaches which are aimed at describing the Cronin effect and high  $p_t$  suppression. Thus, in order to be convinced enough, it is necessary to perform more detailed investigation in the future.

After these phenomenological analyses, we can add numbers on the axes of "phase diagram" in Fig. 3. The results are summarized in Fig. 4, where the diagrams for a proton and a nucleus are shown separately because respective saturation scales are different. Since the saturation scale (squared) for Au is larger than that for a proton by a factor  $A^{1/3} \sim 6$ , the saturation regime for Au is bigger. Kinematically allowed regions for HERA and RHIC are also specified on the figure. Clearly, HERA and forward rapidities at RHIC have large overlapping with saturation regime, while the mid-rapidity at RHIC does not.

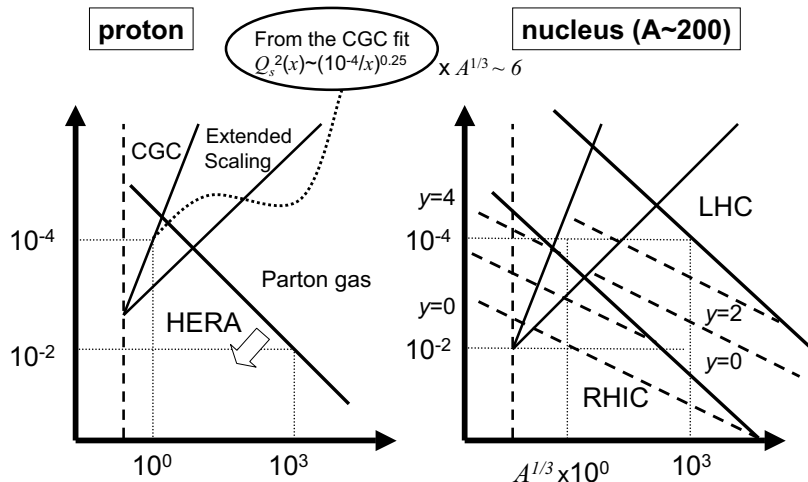


Figure 4. "Phase diagram" with numbers determined from the phenomenological analyses. Vertical and horizontal axes are  $x$  and  $Q^2$  (or  $k_{\perp}^2$  of gluons for a nucleus) in log scale. Kinematically allowed regions are shown for HERA, RHIC and LHC experiments.

### 3.4. CGC at the LHC

Now it is straightforward to draw lines for the LHC on the same phase diagram (number of nucleons for Pb is not so different from that for Au). As is seen in Fig. 4 (right), kinematically allowed region for the LHC has significant overlapping with the saturation



regime even at mid-rapidity. More precisely, for the same transverse momentum, the saturation scale at the LHC is increased by a factor 3 than that of RHIC. Therefore, the effects of saturation is expected to be more visible at the LHC. There are already predictions for the multiplicities for pA and AA collisions [33] and the nuclear modification factor for pA collision [27]. Predictions for other observables are also necessary before the LHC starts to operate. In order to make realistic predictions, we will have to consider both the initial-state (CGC) and final-state (energy loss) effects. Even at the RHIC energy, the similar situation should be seen at forward rapidities in Au-Au collisions. Studying this situation in RHIC will be very helpful to understand the future LHC experiments.

#### 4. Recent progress in theory – Beyond the BK equation

Most recently, there is a growing acceptance that the BK equation is not sufficient to correctly describe the high-energy limit of QCD. Since this was first discussed in detail by Mueller and Shoshi [34], studies of the physics beyond the BK equation is becoming one of the main subjects of the CGC or saturation physics. Research on this subject is still rapidly developing with some (technical and conceptual) problems left unresolved, and it is rather difficult (and even not appropriate) at this time to make a conclusive statement (for references, see the citation list of Ref. [34]: there are 51 hits by now). Instead, I would comment briefly on some general picture which we are aiming at.

Suppose that we have a complete description of the high-energy limit of QCD. It should at least contain pomerons (2 reggeized gluon exchange,  $C$  even), odderons (3 reggeized gluon exchange,  $C$  odd), and reggeons (quark antiquark exchange, etc) as the exchanges between a projectile and a target, and correct interaction among them. On the other hand, the BK equation describes only (multiple exchanges of) pomerons, and pomeron *merging* as the interaction (from the target point of view). This implies that the BK equation is *not symmetric* under the exchange between a target and a projectile. In order to obtain a symmetric picture which also contains other exchanges, we have to go beyond the BK equation. This activity has two different aspects: one is to consider  $n$ -point correlation functions ( $n > 2$ ), and the other is to find correct interactions among the above-mentioned exchanges. Note that the evolution of the CGC can be formulated as a stochastic process governed by a Hamiltonian. Within this context, the pomeron can be described as a kind of two particle collective state (a two point function) of this Hamiltonian. Recently, it has been established that the odderon exchange also appears as the collective state of this Hamiltonian, but is given by a "three particle" state (a three point function) which is odd under charge conjugation [35]. However, this Hamiltonian itself has to be modified because it does not contain the pomeron *splitting*. Inclusion of pomeron splitting to the evolution equation has been discussed by several people. What I can say at present is that we are certainly approaching towards the complete description of the high-energy limit of QCD.

#### REFERENCES

1. J. Breitweg et al. (ZEUS), Phys. Lett. **B487** (2000) 53; S. Chekanov et al. (ZEUS), Eur. Phys. J. **C21** (2001) 443; C. Adloff et al. (H1), Eur. Phys. J. **C21** (2001) 33.
2. S. Eidelman et al. (Particle Data Group), Phys. Lett. **B592** (2004) 1.
3. J.R. Cudell et al. (COMPETE Collab.), Phys. Rev. **D65** (2002) 074024.

4. For a recent review, see E. Iancu and R. Venugopalan, hep-ph/0303204.
5. I. Balitsky, Nucl. Phys. **B463** (1996) 99, Y. Kovchegov, Phys. Rev. **D60** (1999) 034008.
6. E. Levin and K. Tuchin, Nucl. Phys. **A691** (2001) 779.
7. E. Iancu, K. Itakura, and L. McLerran, Nucl. Phys. **A708** (2002) 327.
8. A. Mueller and D. Triantafyllopoulos, Nucl. Phys. **B640** (2002) 331.
9. M. Braun, Eur. Phys. J. **C16** (2000) 337, K. Golec-Biernat, L. Motyka and A.M. Stasto, Phys. Rev. **D65** (2002) 074037, C. Marquet and G. Soyez, Nucl. Phys. **A760** (2005) 208.
10. D. Triantafyllopoulos, Nucl. Phys. **B648** (2003) 293.
11. A. Stasto, K. Golec-Biernat and J. Kwiecinski, Phys. Rev. Lett. **86** (2001) 596.
12. K. Itakura, " *Color Glass Condensate in QCD at High Energy*", hep-ph/0410336, proceedings for ICHEP2004.
13. L. Lipatov, Sov. J. Nucl. Phys. **23** (1976) 338, E. Kuraev, L. Lipatov and V. Fadin, Sov. Phys. JETP, **45** (1977) 199, I. Balitsky and L. Lipatov, Sov. J. Nucl. Phys. **28** (1978) 822.
14. S. Munier and R. Peschanski, Phys. Rev. Lett. **91** (2003) 232001, Phys. Rev. **D69** (2004) 034008, Phys. Rev. **D70** (2004) 077503.
15. K. Golec-Biernat & M. Wüsthoff, Phys. Rev. **D59** (1999) 014017, *ibid.* **D60** (1999) 114023.
16. E. Iancu, K. Itakura and S. Munier, Phys. Lett. **B590** (2004) 199.
17. J. R. Forshaw, R. Sandapen and G. Shaw, Phys. Rev. **D69** (2004) 094013; Phys. Lett. **B594** (2004) 283.
18. V.P. Goncalves and M.V.T. Machado, Eur. Phys. J. **C37** (2004) 299.
19. D. Kharzeev and E. Levin, Phys. Lett. **B523** (2001) 79.
20. T. Hirano and Y. Nara, Nucl. Phys. **A743** (2004) 305.
21. A. Dumitru and J. Jalilian-Marian, Phys. Rev. Lett. **89** (2002) 022301.
22. I. Arsene *et al.* (BRAHMS Collab.), Phys. Rev. Lett. **93** (2004) 242303.
23. D. Kharzeev, Y. Kovchegov, and K. Tuchin Phys. Rev. **D68** (2003) 094013.
24. J. Albacete, N. Armesto, A. Kovner, C. Salgado and U. Wiedemann, Phys. Rev. Lett. **92** (2004) 082001.
25. J. Jalilian-Marian and Y. V. Kovchegov, Prog. Part. Nucl. Phys. **56** (2006) 104.
26. E. Iancu, K. Itakura and D. Triantafyllopoulos, Nucl. Phys. **A742**, 182 (2004).
27. D. Kharzeev, Y. V. Kovchegov and K. Tuchin, Phys. Lett. B **599** (2004) 23.
28. A. Dumitru, A. Hayashigaki and J. Jalilian-Marian, arXiv:hep-ph/0506308.
29. V. Guzey, M. Strikman and W. Vogelsang, Phys. Lett. B **603** (2004) 173.
30. J. Jalilian-Marian, Nucl. Phys. A **739** (2004) 319, Nucl. Phys. A **753** (2005) 307  
M. A. Betemps and M. B. Gay Ducati, Phys. Rev. D **70** (2004) 116005, R. Baier, A. H. Mueller and D. Schiff, Nucl. Phys. A **741** (2004) 358.
31. F. Gelis and R. Venugopalan, Phys. Rev. D **69** (2004) 014019, J. P. Blaizot, F. Gelis and R. Venugopalan, Nucl. Phys. A **743** (2004) 57, H. Fujii, F. Gelis and R. Venugopalan, arXiv:hep-ph/0504047, K. Tuchin, Phys. Lett. B **593** (2004) 66, F. Gelis, K. Kajantie and T. Lappi, these proceedings (arXiv:hep-ph/0509343), D. D. Dietrich, Phys. Rev. D **70** (2004) 105009.
32. D. Kharzeev, E. Levin and L. McLerran, Nucl. Phys. A **748** (2005) 627.
33. D. Kharzeev, E. Levin and M. Nardi, Nucl. Phys. A **747** (2005) 609.
34. Al. Mueller and A. Shoshi, Nucl. Phys. **B692** (2004) 175.
35. Y. Hatta, E. Iancu, K. Itakura, and L. McLerran, Nucl. Phys. **A760** (2005) 172.